

Robust Wide-Range Control of Steam-Electric Power Plants

Chen-Kuo Weng and Asok Ray, *Senior Member, IEEE*

Abstract—To facilitate daily cycling of large electric generating units that were originally designed for baseload operation, the control system has to be redesigned for plant maneuverability over the operating range. A methodology for synthesizing an integrated feedforward-feedback control (FF/FBC) strategy is proposed for wide-range robust control of commercial-scale steam-electric power plants. In the proposed methodology, the feedforward control (FFC) policy is generated via nonlinear programming for simultaneous optimization of all control inputs under specified constraints. This family of optimized trajectories, which represent the best achievable performance of the plant under specified conditions, serve as tracking signals for the FF/FBC system. The feedback control (FBC) law is synthesized following the \mathcal{H}_∞ -based structured singular value (μ) approach to achieve the specified stability and performance robustness. The major features of the integrated FF/FBC system are 1) optimized performance over a wide operating range resulting from the feedforward element and 2) guaranteed stability and performance robustness resulting from the feedback element. To exemplify this control methodology, a family of FFC policies has been synthesized based on a nonlinear state-space model of a 525 MWe fossil-fueled power plant. The synthesis of an FFC policy is identified as an optimization problem where the performance is characterized by rapid maneuvering of electric power to meet the specified load demand while simultaneously maintaining the throttle steam temperature and pressure, and the hot reheat steam temperature within allowable ranges of variation. The results of simulation experiments show that the FF/FBC system satisfies the specified performance requirements of power ramp up and down in the range of 40%–100% load under nominal operating conditions. The results also suggest that this robust control law is capable of rejecting the anticipated disturbances such that the plant closely follows the optimal trajectory determined by the FFC policy. Although this research focuses on control and operation of fossil power plants, the proposed FF/FBC synthesis methodology is also applicable to other complex processes such as planned shutdown of nuclear power plants, take-off and landing of aircraft, and start-up and transient operations of rocket engines.

Index Terms—Feedforward-feedback control, powerplant control, robust control.

I. INTRODUCTION

AUTOMATED process control plays a key role in the continuous search for enhanced safety, reliability and performance of electric power plant operations. The U.S. electric utility industry has recently been confronted with immense technical and financial challenges. These include

Manuscript received March 13, 1995. Recommended by Associate Editor, G. Rogers. This work was supported in part by National Science Foundation Grants ECS-9216386 and DMI-9424587 and Electric Power Research Institute Contract EPRI RP8030-05.

The authors are with the Mechanical Engineering Department, The Pennsylvania State University, University Park, PA 16802 USA.

Publisher Item Identifier S 1063-6536(97)02249-5.

government regulations on the emission standard and intense competition by independent power producers resulting from the Energy Deregulation Act. Moreover, the aging utility-owned power generating units already have high operation and maintenance costs. Nearly 70% of U.S. fossil power plants, representing more than 45% of U.S. electric power generation capacity, will be over 30 years old by the year 2000. Since most of these plants are designed for a service life of 40 years, a significant part of their useful life is already expended. Therefore, in order to extend the remaining service life, the utility companies will have to carefully operate and maintain these aging power plants to avoid forced shutdown while simultaneously matching varying load demand and meeting increased competition for lower cost of electricity. For example, in the load following mode of a fossil power plant, excursions of the main steam and reheat steam temperature and pressure must be regulated within prescribed limits to ensure plant safety (e.g., protection of the steam headers and turbines). Daily cycling of large generating units that were originally designed for baseload operations has now become an economic necessity for many utility companies [2], [7]. The power plant control system, under these circumstances, must allow rapid load maneuvering without violating the constraints of temperature and pressure oscillations in order to avoid excessive stresses on the plant components [10].

The concepts of both feedforward (open-loop) and deterministic feedback (closed-loop) control have been adopted in this paper. A feedforward control (FFC) system can achieve the best nominal performance under specified constraints based on a given performance index and a plant model but it has limited capability to tolerate disturbances and malfunctions which are not included in the plant model. For example, under open-loop control, a change in the valve characteristics due to sticking will cause a variation in valve position in response to a given input-demand signal, thus introducing an error into the performance of the open-loop control [11]. Such disturbances may even cause plant instability, and the control system will not be able to compensate for these disturbances without appropriate feedback actions. The feedback control (FBC) adjusts the inputs to the plant based on the difference between the input demand signals and the measured plant outputs. With this structure, FBC has the capability to overcome uncertainties and perturbations in the control system.

The control system for wide-range operations has been synthesized by combining FFC with FBC to provide good performance and ability to overcome exogenous disturbances and plant modeling uncertainties. The resulting control structure is commonly called integrated feedforward-feedback control

(FF/FBC). With this structure, the FFC maneuvers the plant trajectory close to the desired operating conditions, and only a smaller range of actions is left for the FBC to compensate. Therefore, the performance of FF/FBC is anticipated to be better than FFC or FBC alone. Since FBC can attenuate the errors induced by perturbations, the FF/FBC system can overcome a larger set of disturbances. The most effective control strategy under the current state-of-the-art of power plant operations is the integrated control system, which combines a number of classical (e.g., single-input/single-output lead-lag and proportional-integral-derivative) FBC's and static FFC's separately designed for each subsystem. Since the main function of the FFC in the FF/FBC structure is to ensure good nominal performance, the nonlinear programming technique that optimizes the plant dynamic performance based on a specified cost functional and constraints has been adopted to generate the FFC input sequence. On the other hand, the major objective of the FBC is to provide good stability and performance robustness. Hence, the \mathcal{H}_∞ -based structured singular value (μ) technique that synthesizes multiple-input/multiple-output (MIMO) feedback control laws with guaranteed robustness is adopted here. In the conventional control systems design, the nominal trajectory is unknown and the FBC attempts to regulate the plant response during the transients as close to the final steady-state set point as possible. On the contrary, in the proposed approach, the nominal trajectory is known *a priori* and is fed into the control loop as a tracking signal. The FBC is only required to subdue the disturbances to follow the nominal trajectory generated by the FFC.

The power plant under consideration is a fossil-fueled, generating unit having the rated capacity of 525 MWe. The plant dynamics have been represented by a 27th-order nonlinear state-space model which is described in detail by Ray and Weng [8] and Weng [13]. The plant maintains the throttle steam condition at 2415 psia (16.65 MPa) and 950° F (510°C), and hot reheat steam temperature at 1000° F (537.8°C). The following four valve commands are selected as control inputs: (high-pressure turbine) governor valve area (AGVR), feedpump turbine speed control valve area (APTR), fuel/air valve area (AFAR), and reheat spray attemperator valve area (AATR). The measured plant outputs are electric power (JGN), throttle steam temperature (THS), hot reheat steam temperature (THR), and throttle steam pressure (PHS). The control problem is to steer the plant from the initial equilibrium state of power at 525 MWe (100% load) to the new equilibrium state of 210 MWe (40% load) within a specified time and without violating the prescribed constraints. The objective is to facilitate daily cycling of large electric generating units that were originally designed for baseload operation. In the proposed control synthesis methodology, the FFC law is generated via nonlinear programming (NP) for simultaneous optimization of all control inputs under specified constraints. This family of optimized trajectories, which represent the best achievable performance of the plant under the specified conditions, serve as tracking signals for the FF/FBC system. The FBC law is synthesized following the \mathcal{H}_∞ -based structured singular value (μ) approach to achieve the desired stability and performance robustness.

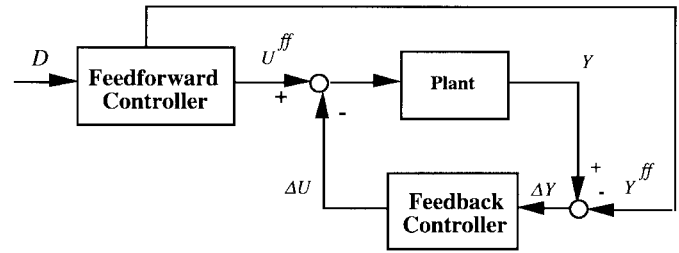


Fig. 1. The proposed FF/FBC structure.

The structure of the proposed FF/FBC system is shown in Fig. 1. The FFC input U^{ff} and the corresponding plant output Y^{ff} , which are calculated off-line by NP, are used as the reference control input and tracking signals, respectively; and ΔY and ΔU are the inputs and outputs of the FBC. In the presence of disturbances, the actual trajectory may deviate from the nominal trajectory, and the role of FBC is to compensate for this deviation. The contributions of the research work reported in this paper are summarized below:

- formulation of a methodological framework for synthesizing a robust FF/FBC strategy for wide-range operations of complex dynamic processes using the recent developments in the systems theory with specific applications to commercial-scale electric power plants;
- optimization of nominal plant trajectories of a power plant under a variety of operating conditions corresponding to load cycling, hot start-up, and scheduled shutdown;
- formulation of a methodology for synthesizing robust controllers for wide-range operations of complex thermo-fluid-mechanical processes, which can also accommodate multiobjective optimization of additional performance requirements such as life extension and damage mitigation.

This paper is organized in five sections and an Appendix. Section II formulates the FFC synthesis problem in the setting of nonlinear programming. Section III presents the problem formulation and synthesis of the FBC law in the μ -setting supported by a brief review of the fundamental properties of the structured singular value (μ) in the Appendix. Section IV presents the results of simulation experiments conducted on the nonlinear dynamic model under the proposed FF/FBC. Finally, Section V summarizes and concludes the paper.

II. SYNTHESIS OF THE OPTIMAL FEEDFORWARD CONTROL POLICY

The NP problem for the optimal FFC is formulated in the following generic form:

$$\begin{aligned}
 \text{(NP)} \quad & \text{Minimize} && J(u) \\
 & \text{subject to} && g_i(u) \leq 0 \quad \text{for } i = 1, \dots, m \\
 & && h_j(u) = 0 \quad \text{for } j = 1, \dots, p \quad (1)
 \end{aligned}$$

where u is the set of decision variables, $J(u)$ is the objective functional reflecting the mission goal, $g_i(u) \leq 0$ represents the set of inequality constraints related to the plant operating conditions, and the set of equality constraints $h_j(u) = 0$ represents the plant dynamics. Each of $J(u)$, $g_j(u)$ and $h_j(u)$ in (1) is allowed to be smooth nonlinear functions of the decision variables u .

The task of FFC synthesis in this paper is to optimize the feedforward input sequence as a decision law U^{ff} over a given finite-time horizon. The FFC law has been synthesized in the discrete-time setting as a standard NP problem whose solution is a sequence $U^{ff} = \{u_0, u_1, \dots, u_{n-1}\}$; the subscripts 0 and n correspond to the initial time and the final time, respectively. The plant output $Y^{ff} = \{y_1, y_2, \dots, y_n\}$ is the corresponding output sequence where y_0 is specified as a known initial condition. The control input u_n at the final n th step is not included in the sequence U^{ff} because the optimization problem has no bearing on the control input at the final time. The objective functional $J(u)$ is selected to represent a performance measure of plant operations under the FFC policy over the finite time horizon of interest, and the constraints that specify the feasibility of the NP problem are chosen to delineate the plant dynamics, the region of desired plant operation, and the physical limitations. In the discrete-time setting, the FFC optimization problem is formulated as follows:

$$\begin{aligned}
 \text{(NP) Minimize} \quad & J = \sum_{k=1}^N [\tilde{y}_k^T Q_k \tilde{y}_k + \tilde{u}_{k-1}^T \tilde{u}_{k-1}] \Delta t_k \\
 \text{subject to} \quad & x_{k+1} = x_k + \int_{t_k}^{t_{k+1}} f(x, u) dt \\
 & u_k - u_k^{ub} \leq 0; \quad \text{and} \quad u_k^{lb} - u_k \leq 0 \\
 & g_k(x_k, u_k) \leq \beta_k
 \end{aligned} \tag{2}$$

where the plant output y_k is a function of the plant state x_k and the control input u_k , i.e., $y_k = q(x_k, u_k)$, $\tilde{y}_k = y_k - y_{sk}$ is the deviation of the plant output y_k from the respective desired values y_{sk} at time t_k , $\tilde{u}_k = u_k - u_{sk}$ is the deviation of u_k from the respective desired values u_{sk} , the performance objective functional $J(u)$ is a weighted ℓ_2 norm of \tilde{y}_k and \tilde{u}_k , which signifies the total mean-square error, the weighting matrices Q_k and R_k serve as the relative weights between the variations of \tilde{y}_k and \tilde{u}_k , respectively, the equality constraint $x_{k+1} = x_k + \int_{t_k}^{t_{k+1}} f(x, u, t) dt$ satisfies the nonlinear model of plant dynamics, $\{u_k^{ub}\}$ and $\{u_k^{lb}\}$ are the sequences of the upper and lower bounds within which the control inputs are constrained, and β_k is the upper bound of $g_k(x_k, u_k)$ which represents the selected plant variables or their combinations. N is the total number of discrete steps from the initial time, t_0 , to the final time t_f ; and Δt_k is the possibly nonuniform time interval, $\Delta t_{k+1} = t_k - t_{k-1}$, for $k = 1, 2, \dots, N$, which must be chosen properly. If the time intervals are too large, the performance of FFC will degrade; conversely, if they are too small, more steps are required and the number of decision variables becomes large.

A. Formulation of the Objective Functional

The goal of the FFC is to have rapid response to changes in load demand while maintaining the plant output variables (e.g., THS and PHS) constant. Consequently, the performance measure is expressed in terms of the rate of load change, deviations in plant variables, and rate of change of actuator commands. Load change rates were specified according to the needs of the utility industry. Referring to the standard of Electric Power Research Institute (EPRI) [10], the target load change rate was set to a ramp up or down at 10% of the rated load of 525 MWe/min, i.e., 52.50 MWe/min, in the 100%

TABLE I
SELECTED WEIGHTS IN THE OBJECTIVE FUNCTIONAL

Variable y_k	JGN	THS	THR	PHS
Values of Q_k	25.0	0.25	0.10	0.01
Variable u_k	AGVR	APTR	AFAR	AATR
Values of R_k	1.0	1.0	1.0	1.0

to 40% load range. On the other hand, in order to maintain high efficiency and reduce material damage, throttle steam temperature and pressure, and hot reheat steam temperature has to be maintained as close to their respective nominal values as possible. The desired load trajectory is a 52.5 MWe/min ramp (up or down) rate power output while reducing the oscillations of the plant variables as much as possible. That is, the desired values of y_{sk} at time t_k are the following:

- $(\text{JGN})_k$ = the value of the power rate corresponding to the specified ramp rate;
- $(\text{THS})_k = 950^\circ\text{F}$ (510°C);
- hot reheat steam temperature $(\text{THR})_k = 1000^\circ\text{F}$ (537.8°C);
- $(\text{PHS})_k = 2415$ psia (16.65 MPa).

Since oscillations of the valve actuators contribute to the wear and tear of the moving components, the rate of the control valve movement is penalized. Accordingly, u_{sk} is set to u_{k-1} with u_{-1} equal to the known control input prior to initiation of the load ramp. Furthermore, the control inputs u_k are constrained to satisfy the physical limitations of the actuators. Since the plant parameters do not vary over the time horizon of interest, the weighting matrices Q_k and R_k were chosen as constant diagonal matrices. Further, since the plant model is required to follow a transient trajectory, the time intervals Δt_k in the objective functional of (2) were chosen to be uniformly spaced over the entire time horizon with the size equal to 1 s, i.e., $\Delta t_k = 1$ s, for all k .

Table I lists the (diagonal) elements of the output and control weighting matrices Q_k and R_k . Each (diagonal) element of the control weighting matrix R_k is chosen to be one because each actuator command is normalized. On the other hand, the (diagonal) entries of the output weighting functions Q_k are chosen to reflect the relative importance for each variable. In order to closely follow the desired power output at a specified rate of ramp up or down, the weight on JGN is selected to be the largest. The values of Q_k 's for the remaining three outputs are accordingly selected with reference to their respective allowable variations, in which the outputs with smaller allowable variations are selected to have higher weights. For example, the THS is weighted more heavily than the hot reheat temperature THR because fluctuations in THR is relatively less harmful to the steam headers and turbine blades than those in THS. Similarly, the throttle steam pressure PHS is weighted the least because a pressure swing is considered to have less harmful effects on structural integrity of the power plant than an equivalent temperature swing. However, there are no firm rules for selection of the weighting matrices Q_k and R_k ; these are largely the choice of the plant operation engineer.

B. Specification of Constraints

Since physical limitations such as actuator saturation are always present in the real world, the nonlinear programming approach may not yield a practical solution of an FFC policy unless appropriate constraints are specified. In this FFC synthesis problem, the constraints are classified into the following two categories, namely, physical constraints and operational constraints.

- *Physical constraints:* These constraints represent the physical limitations of the process dynamics. For example, a valve can only have a position from fully open (100%) to fully closed (0%). Therefore, physical constraints are critical for process optimization and cannot be violated. The physical constraints considered in this FFC problem are the four control valve areas. Since, in this problem, the decision variables are chosen to be the control inputs, these physical constraints are simply specified as the upper and lower bounds.
- *Operational constraints:* Although these constraints are physically possible, they are imposed on the FFC synthesis problem for specific purposes such as to enhance safety and performance of the control system. For example, the steam temperatures are restricted to remain below a certain level to avoid possible creep damage in the headers and thermal shock in the turbine blades. The tolerable variations of the measured outputs, namely, THS, THR, and PHS, are specified as: THS within $\pm 10^\circ\text{F}$ (5.56°C); THR within $\pm 15^\circ\text{F}$ (8.33°C), and PHS within ± 45 psi (0.310 MPa) [7].

C. Numerical Computation of the Feedforward Control (FFC) Policy

The optimization of the FFC strategies was accomplished by the nonlinear programming NP software package NPSOL [5] on a Silicon Graphics Indy computer workstation. NPSOL uses the sequential quadratic programming (SQP) algorithm which has been shown to outperform many other tested methods in terms of computational efficiency, accuracy, and percentage of successful solutions over a large number of test problems [9], [12]. The basic algorithm of the SQP technique is to approximate a general NP problem as a sequence of quadratic programming (QP) problems, and then to use the solution obtained from one QP problem as the search direction for the next QP problem. At each iteration starting from the current point x , the new iterate point is obtained as $\bar{x} = x + \alpha \delta x$ where δx is the solution of the previous QP problem serving as the search direction and $\alpha > 0$ is the scale factor for adjusting the correction. Each iteration involves two series of iterations, namely major iterations and minor iterations. In the major iterations, α is determined by minimizing a suitable merit function and δx is determined from the minor iterations. Merit functions are used to enforce steady progress toward the optimal point by balancing the (usually) conflicting aims of reducing the objective functional and satisfying the nonlinear constraints [5].

The variable-step Runge–Kutta–Fehlberg method [4] has been adopted for the integration of nonlinear differential

equations of the dynamic plant model. The numerical solution of the above NP problem for constrained optimization of the power plant performance is computationally intensive. Specifically, in this FFC synthesis problem, the target load change rate is 10%/min (i.e., the elapse time of the control process from 100% to 40% is 6 min) and the time interval between the consecutive instants of control updating is equal to 1 s (i.e., the control inputs have to be updated at 360 discrete instants of time). With four control inputs at each time step, the FFC synthesis problem requires a total of 1440 decision variables to be optimized. The required central processing unit (CPU) time for computing this problem on a state-of-the-art workstation computer (e.g., Silicon Graphics Indy) is estimated to be in order of tens of days. Therefore, an alternative formulation must be used to enhance the speed of computation.

The CPU time (T) required to solve an NP problem is approximately proportional to a polynomial function of the number of the decision variables, $N_D = N \times m$ where N is the number of steps and m is the dimension of the control input u in the optimization problem. Therefore, reduction of N_D in the formulation of the NP problem is one of the most effective ways to circumvent the difficulty of time-consuming calculations. As the desired optimal trajectory is known, the NP problem can be divided into a number of smaller dimensional subproblems, each of which is used to optimize the control input sequence for the respective section of the optimal trajectory. Then, the complete sequence of control inputs can be obtained as a suboptimal solution by concatenating the solutions of each subproblem. For a problem being divided into M subproblems, each with $N_{D_{\text{sub}}} = N_D/M$ decision variables, the total CPU time is approximately reduced by a factor of some power of M . In this paper, the FFC problem has been divided into 20 subproblems. In each subproblem, the power output is reduced by 3% (15.75 MWe) at the rate of 10%/min (i.e., the subproblem is solved for a period of 18 s). Therefore, selecting the uniformly spaced time interval in the objective functional of (2) to be 1 s (i.e., $\Delta t_k = 1$ for all k), the number of decision variables to be identified in each subproblem becomes $N_{D_{\text{sub}}} = 18 \times 4 = 72$. In this formulation, the optimization for each subproblem needs about 5 h CPU time on a Silicon Graphics Indy, and the total CPU time for computing the 20 subproblems is about 100 h. Although the resulting FFC trajectories are obtained as suboptimal solutions, they adequately serve as reference trajectories for load cycling, automated start-up, and scheduled shutdown in power plants. The specifications for the n th subproblem in this problem are summarized below.

(NP) Minimize the cost functional in (2)

$$J_n = \sum_{i=1}^{18} \{ Q_{1i}(\text{THS} - 950)^2 + Q_{2i}(\text{THR} - 1000)^2 + Q_{3i}(\text{PHS} - 2415)^2 + Q_{4i}(\text{JGN} - y_{\ell(n,i)})^2 + R_{1i}(u_{1,i} - u_{1,i-1})^2 + R_{2i}(u_{2,i} - u_{2,i-1})^2 + R_{3i}(u_{3,i} - u_{3,i-1})^2 + R_{4i}(u_{4,i} - u_{4,i-1})^2 \} \quad (3)$$

subject to

TABLE II
SYSTEM EIGENVALUES AT DIFFERENT LOAD LEVELS

100% load	90% load	80% load	70% load
-21.0829	-21.4011	-21.7782	-22.1945
-17.1988	-14.8868	-12.3836	-9.3068
-4.3653 + 0.6651i	-4.4649 + 0.5953i	-4.8802	-6.3158
-4.3653 - 0.6651i	-4.4649 - 0.5953i	-4.3700	-3.6448
-2.9839	-3.0614	-3.1465	-3.3566
-2.1417	-2.1641	-2.1881	-2.2139
-1.6282	-1.6377	-1.6508	-1.6712
-1.0895	-1.0777	-1.0867	-1.1329
-1.0003	-1.0016	-1.0017	-1.0017
-0.6750 + 0.2513i	-0.6468 + 0.2396i	-0.6221 + 0.2191i	-0.6000 + 0.1822i
-0.6750 - 0.2513i	-0.6468 - 0.2396i	-0.6221 - 0.2191i	-0.6000 - 0.1822i
-0.6994	-0.6475	-0.6009	-0.5608
-0.2832 + 0.1065i	-0.2740 + 0.1019i	-0.2649 + 0.0963i	-0.3031
-0.2832 - 0.1065i	-0.2740 - 0.1019i	-0.2649 - 0.0963i	-0.2558 + 0.0894i
-0.3228	-0.3171	-0.3106	-0.2558 - 0.0894i
-0.1576 + 0.1168i	-0.1480 + 0.1128i	-0.1387 + 0.1072i	-0.1295 + 0.0998i
-0.1576 - 0.1168i	-0.1480 - 0.1128i	-0.1387 - 0.1072i	-0.1295 - 0.0998i
-0.1625	-0.1531	-0.1436	-0.1331
-0.0396 + 0.0753i	-0.0358 + 0.0694i	-0.0320 + 0.0631i	-0.0279 + 0.0568i
-0.0396 - 0.0753i	-0.0358 - 0.0694i	-0.0320 - 0.0631i	-0.0279 - 0.0568i
-0.0082	-0.0075	-0.0067	-0.0059
-0.0522	-0.0476	-0.0188	-0.0167
-0.0228	-0.0208	-0.0432	-0.0390
-0.0313	-0.0291	-0.0268	-0.0243
-20.0000	-20.0000	-20.0000	-20.0000
-20.0000	-20.0000	-20.0000	-20.0000
-3.3330	-3.3330	-3.3330	-3.3330
60% load	50% load	40% load	35% load
-22.6994	-23.3030	-24.0648	-24.6146
-6.8999 + 2.2225i	-5.9208 + 2.5743i	-6.4895	-8.1803
-6.8999 - 2.2225i	-5.9208 - 2.5743i	-4.0522	-2.0899 + 3.0406i
-3.3198 + 0.4576i	-3.1898 + 0.8027i	-2.9079 + 2.4263i	-2.0899 - 3.0406i
-3.3198 - 0.4576i	-3.1898 - 0.8027i	-2.9079 - 2.4263i	-3.5611
-2.2417	-2.2731	-2.3337	-2.3685
-1.7121	-1.8486	-2.0509	-2.0170
-1.2530	-1.4678	-1.5994	-1.6311
-1.0017	-1.0017	-1.0007	-1.0006
-0.5689 + 0.1081i	-0.6807	-0.7288	-0.7431
-0.5689 - 0.1081i	-0.4574 + 0.0598i	-0.3861 + 0.0386i	-0.3479
-0.5431	-0.4574 - 0.0598i	-0.3861 - 0.0386i	-0.3634
-0.2942	-0.2819	-0.2643	-0.2522
-0.2469 + 0.0810i	-0.2384 + 0.0712i	-0.2305 + 0.0607i	-0.2268 + 0.0563i
-0.2469 - 0.0810i	-0.2384 - 0.0712i	-0.2305 - 0.0607i	-0.2268 - 0.0563i
-0.1203 + 0.0903i	-0.1107 + 0.0782i	-0.0999 + 0.0633i	-0.0936 + 0.0543i
-0.1203 - 0.0903i	-0.1107 - 0.0782i	-0.0999 - 0.0633i	-0.0936 - 0.0543i
-0.1222	-0.1104	-0.0971	-0.0896
-0.0239 + 0.0498i	-0.0197 + 0.0424i	-0.0153 + 0.0348i	-0.0130 + 0.0309i
-0.0239 - 0.0498i	-0.0197 - 0.0424i	-0.0153 - 0.0348i	-0.0130 - 0.0309i
-0.0050	-0.0043	-0.0037	-0.0034
-0.0146	-0.0124	-0.0102	-0.0091
-0.0350	-0.0319	-0.0298	-0.0290
-0.0218	-0.0190	-0.0161	-0.0146
-20.0000	-20.0000	-20.0000	-20.0000
-20.0000	-20.0000	-20.0000	-20.0000
-3.3330	-3.3330	-3.3330	-3.3330

$$x_{k+1} = x_k + \int_{t_k}^{t_{k+1}} f(x, u, t) dt$$

$$0 \leq u_k \leq 1$$

$$940^\circ\text{F} \leq \text{THS} \leq 960^\circ\text{F}$$

$$985^\circ\text{F} \leq \text{THR} \leq 1015^\circ\text{F}$$

$$2370 \text{ psi} \leq \text{PHS} \leq 2460 \text{ psi}$$

$$-0.5\%/s \leq \text{JGN} \leq 0\%/s$$

where $\ell(n, i) = 18(n-1) + i$; Y_ℓ represents the desired power output at time $t_\ell = \ell$ th instant. Referring to Table I, the weights for plant output variables are specified as $Q_{1i} =$

25.0 , $Q_{2i} = 0.25$, $Q_{3i} = 0.10$, and $Q_{4i} = 0.01$, for $i = 1, \dots, 14$. In order that the nominal trajectory (i.e., the plant trajectory in the absence of any disturbances) converges toward the terminal point of the desired trajectory, the weights at the last four time intervals ($i = 15, \dots, 18$) were increased to 100 times the weights at the first eight intervals, that is, $Q_{1i} = 2500.0$, $Q_{2i} = 25.0$, $Q_{3i} = 10.0$, and $Q_{4i} = 1.0$ for $i = 15, \dots, 18$. The weights for control input variables, however, are held constant at $R_{1i} = 1.0$, $R_{2i} = 1.0$, $R_{3i} = 1.0$, and $R_{4i} = 1.0$ for $i = 1, \dots, 18$, as specified in Table I. Furthermore, the instantaneous rate of power change was

TABLE III
TRANSMISSION ZEROS AT DIFFERENT LOAD LEVELS

100% load	90% load	80% load	70% load
-14.6784	-13.7896	-12.9703	-12.2117
-5.6242 + 0.9839i	-5.4202 + 1.9180i	-5.1196 + 2.6050i	-4.7112 + 3.1906i
-5.6242 - 0.9839i	-5.4202 - 1.9180i	-5.1196 - 2.6050i	-4.7112 - 3.1906i
1.5408 + 2.3743i	1.8443 + 2.3390i	2.1653 + 2.2215i	2.4938 + 1.9983i
1.5408 - 2.3743i	1.8443 - 2.3390i	2.1653 - 2.2215i	2.4938 - 1.9983i
-2.1378	-2.1605	-2.1852	-2.2122
-1.6303	-1.6395	-1.6474	-1.6537
-0.0656 + 0.7162i	-0.0492 + 0.6763i	-0.0332 + 0.6449i	-0.0173 + 0.6214i
-0.0656 - 0.7162i	-0.0492 - 0.6763i	-0.0332 - 0.6449i	-0.0173 - 0.6214i
-0.7313	-0.6747	-0.6199	-0.5648
-0.3895 + 0.1274i	-0.3840 + 0.1251i	-0.3772 + 0.1225i	-0.3686 + 0.1192i
-0.3895 - 0.1274i	-0.3840 - 0.1251i	-0.3772 - 0.1225i	-0.3686 - 0.1192i
-0.1423 + 0.1627i	-0.1267 + 0.1501i	-0.1116 + 0.1366i	-0.0969 + 0.1226i
-0.1423 - 0.1627i	-0.1267 - 0.1501i	-0.1116 - 0.1366i	-0.0969 - 0.1226i
-0.0124	-0.0120	-0.0115	-0.0110
-0.0233	-0.0212	-0.0190	-0.0168
-0.0338	-0.0313	-0.0286	-0.0258
60% load	50% load	40% load	35% load
-11.5110	-10.8591	-10.3046	-10.0419
-4.1909 + 3.6960i	-3.5498 + 4.1239i	-2.7851 + 4.4200i	-2.3141 + 4.5632i
-4.1909 - 3.6960i	-3.5498 - 4.1239i	-2.7851 - 4.4200i	-2.3141 - 4.5632i
2.8108 + 1.6319i	3.1056 + 0.9814i	4.5205	5.0065
2.8108 - 1.6319i	3.1056 - 0.9814i	2.2417	1.8937
-2.2422	-2.2747	-2.3106	-2.3334
-1.6570	-1.6541	-1.6430	-1.6347
0.0021 + 0.6073i	0.0286 + 0.6027i	0.0718 + 0.6098i	0.1094 + 0.6231i
0.0021 - 0.6073i	0.0286 - 0.6027i	0.0718 - 0.6098i	0.1094 - 0.6231i
-0.5077	-0.4485	-0.3855	-0.3525
-0.3580 + 0.1149i	-0.3444 + 0.1079i	-0.3278 + 0.0964i	-0.3189 + 0.0866i
-0.3580 - 0.1149i	-0.3444 - 0.1079i	-0.3278 - 0.0964i	-0.3189 - 0.0866i
-0.0827 + 0.1079i	-0.0690 + 0.0925i	-0.0556 + 0.0765i	-0.0486 + 0.0681i
-0.0827 - 0.1079i	-0.0690 - 0.0925i	-0.0556 - 0.0765i	-0.0486 - 0.0681i
-0.0103	-0.0094	-0.0084	-0.0077
-0.0146	-0.0123	-0.0100	-0.0088
-0.0230	-0.0200	-0.0169	-0.0152

constrained between $-0.35\%/s$ (-1.8375 MWe/s) to $0\%/s$ during ramp down and between $+0.35\%/s$ ($+1.8375$ MWe/s) to $0\%/s$ during ramp up so that the profile of actual power does not significantly deviate from the desired ramp rate of $-0.17\%/s$ ($-10\%/min$) and $+0.17\%/s$, respectively.

III. SYNTHESIS OF ROBUST FEEDBACK CONTROL VIA μ

The FBC law is synthesized by the H_∞ -based structured singular value (μ) approach which is briefly described in the Appendix. Since the μ -analysis and synthesis is a linear method, the nonlinear plant model is linearized at a series of steady-state operating points ranging from 100% down to 35% load. This family of linearized plant models provide ample information for selecting a nominal model for control systems synthesis and determining the bounds of errors resulting from linearization. The system eigenvalues (poles) and transmission zeros of each of the linearized systems are listed in Tables II and III, respectively. It is observed that all system eigenvalues of each of the linearized models are located in the left-half s plane. Therefore, each of these linearized models is internally stable, which guarantees stabilizability and detectability as required for H_∞ control synthesis. That is, any possible uncontrollable and unobservable modes will not cause any instability. Although it is not required for FBC synthesis, the above linearized models were tested and found to be completely controllable and observable. It is seen in Table II

that some of the eigenvalues vary significantly with load exhibiting nonlinear nature of the plant dynamics. Also, for each linearized model, some of the transmission zeros lie in the right-half s plane. This implies that the plant model is nonminimum phase and, therefore, the achievable performance of the control system is restricted due to the fact that these right-half s plane zeros cannot be canceled by pole placement. Consequently, for this plant, the task of FBC synthesis is not expected to be straightforward.

A. Identification of Uncertainties

In the μ framework, robustness of the synthesized controller is governed by the specification of the uncertainties. An incorrectly defined uncertainty specification will result in an improper control law. For example, an overestimated uncertainty specification will degrade the performance of the resulting control law; on the contrary, an underestimated uncertainty specification may lead to a control system with inadequate robustness. In the FBC synthesis problem, the uncertainties have been characterized in the additive form in which the relation between the actual plant $\bar{G}(s)$ and the nominal plant $G(s)$ can be expressed by

$$\bar{G}(s) = G(s) + \Delta(s) \quad (4)$$

where $\Delta(s)$ is the additive uncertainty representing possible discrepancy between the actual plant $\bar{G}(s)$ and the nominal

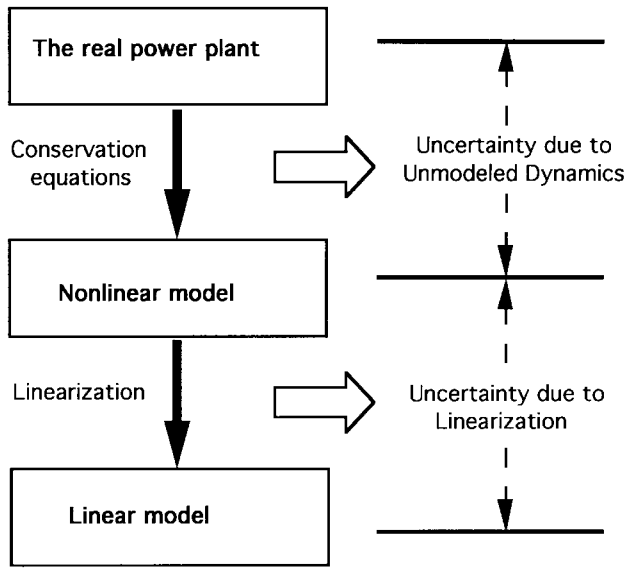


Fig. 2. Uncertainties between the real plant and models.

plant model $G(s)$. The specification of the uncertainties $\Delta(s)$ consists of two components, namely, the weighting function $W_{\text{del}}(s)$ and the normalized perturbation matrix $\Delta_{\text{del}}(s)$ with unity H_∞ norm (i.e., $\|\Delta_{\text{del}}(s)\|_\infty = \sup_\omega \bar{\sigma}(\Delta(j\omega)) \leq 1$). Therefore, $\Delta(s)$ can be expressed as

$$\Delta(s) = W_{\text{del}}(s)\Delta_{\text{del}}(s) \quad (5)$$

where the weighting function $W_{\text{del}}(s)$ denotes the maximum magnitude of $\Delta(s)$ and the normalized perturbation matrix $\Delta_{\text{del}}(s)$ defines the structure of $\Delta(s)$. Unlike the H_∞ approach, in which only the bound of uncertainty $\Delta(s)$ is defined and is assumed to have a full block structure, the structure of uncertainties in the μ approach is formulated in the block diagonal format as $\Delta_{\text{del}}(s) = \text{diag}[\Delta_1(s)\Delta_2(s)\cdots\Delta_n(s)]$. The structure of uncertainties can be described in a more precise manner in this setting and, therefore, the synthesis is less conservative. However, if the uncertainty structure is made more relaxed [e.g., a full block structure of $\Delta_{\text{del}}(s)$], then the control system would become more conservative. In the extreme case where the structure of uncertainties is completely unknown (i.e., full block), μ of the control system is identically equal to its largest singular value which in turn induces a more conservative design. From the above discussion, it is clear that a good μ synthesis strongly relies on the specification of uncertainties. In this research, the major uncertainties considered in the FBC synthesis are the difference between the nominal model and the actual plant. The conceivable discrepancy between the nominal plant model and the actual plant is illustrated in Fig. 2. These are the common uncertainties encountered in a linear feedback control design. The method for quantifying these uncertainties are discussed below.

Since no mathematical model exactly represents a real physical system, there will inevitably be a mismatch between the model prediction and the actual process behavior. In the presence of significant modeling inaccuracies, the performance of a control system will be degraded and may even be unstable.

TABLE IV
UNCERTAINTY SPECIFICATIONS FOR UNMODELED PLANT DYNAMICS

Frequency range (rad/sec)	Percentage of uncertainty magnitude
$< 10^{-3}$	$\pm 5\%$
$10^{-3} \sim 10^{-2}$	$\pm 10\%$
$10^{-2} \sim 10^{-1}$	$\pm 40\%$
$10^{-1} \sim 10^1$	$\pm 80\%$
$> 10^1$	- 90% ~ 200%

Consequently, model mismatch is a crucial issue for control synthesis. The nonlinear model used to represent the thermo-fluid dynamics of the power plant [8], [13] is derived using the lumped parameter approximation in which the high-frequency dynamics of the process are largely neglected. These induced discrepancies can be categorized as unmodeled dynamics. For the nonlinear model, since the steady-state conditions have been verified to match the heat balance data of the power plant and the model parameters of mass, momentum, and energy storage are identified based on the physical principles and actual dimensions of the plant components, the disagreement between the low-frequency responses of the model and the plant is expected to be small. However, in the high-frequency region, the discrepancy between the model and the plant is likely to increase with frequency due to the lumped-parameter nature. Thus, the uncertainties due to unmodeled dynamics are expected to be dominant in the high-frequency region in which the magnitude plot of each plant transfer function can be enclosed by its respective envelope [8], [13].

Based on the above discussion, it is reasonable to assume that the percentage of the uncertainty magnitude is monotonically increasing with frequency. In this design, the associated uncertainty percentages in different frequency ranges are listed in Table IV. The size (i.e., H_∞ norm) of the uncertainty due to unmodeled dynamics is increased from 5% to 200% of the size of the nominal plant model across the frequency range from 10^{-3} to 10^2 rad/s which covers the plant dynamics of interest. When the frequency is lower than 10^{-3} rad/s, the uncertainty size is 5% reflecting an upper bound of the plant modeling error at steady state. In contrast, above 10 rad/s, the relative uncertainty is specified in the range from -90% to 200% reflecting possible (lumped parameter) modeling inaccuracy in the high-frequency range. The physical interpretation of this specification is that, during transient (frequency > 10 rad/s) operations, a unit change of an output variable predicted by the nonlinear model implies that the real output change in the physical plant can lie between 1/10 to 3 units. For example, a high-frequency pressure disturbance of 10 psi amplitude predicted by the nonlinear model may actually be a disturbance of amplitude anywhere between 1–30 psi in the plant.

Another type of uncertainty considered in this research arises from linearization. Since the FBC design is based on the nominal plant model linearized at a specific operating point, the mismatch between the nonlinear model and the nominal linearized model has to be taken into account in addition to the uncertainty due to unmodeled dynamics. Since nonlinear

B. Specification of Performance

Typical time-domain performance criteria that are used to characterize the transient response to a unit step input include overshoot, delay time, rise time, and settling time, etc. In robust feedback control theories, there are no unified methods to synthesize control laws that fulfill the given time-domain specifications. Instead, there are a wide variety of frequency-domain methods available and are suitable for analysis and synthesis of finite-dimensional linear time-invariant control systems. Fortunately, a few time-domain properties can be interpreted in terms of frequency-domain properties based on the relationships that exist between their characteristics. For instance, since steady-state error is almost unavoidable, one common objective for controller design is to keep the error to a minimum, or below a certain tolerance level. The most well-known use of μ for robustness analysis and synthesis is in the frequency domain. In general, there is no direct way to indicate the time-domain performance in the μ synthesis problem because it cannot be directly related to the frequency-domain properties. Perturbations and exogenous disturbances may lead to tracking and regulation errors in a control system. In this FBC design, the steady-state tracking error is specified as one of the performance criteria. Since the steady-state error of a control system is associated with its zero frequency gain, this performance criterion can be specified in the frequency domain under the μ mechanism.

For feedback control synthesis, in addition to the requirement of robust stability, the designer is generally interested in ensuring the time-domain performance requirements (e.g., response time, overshoot, and steady-state errors). In most cases, long before the onset of instability, the closed-loop performance would degrade to the point of unacceptability. Consequently, it is critical to ensure that the requirements for stability and performance are satisfied under specified perturbations. The traditional approach to test the robustness properties is to conduct simulation experiments to identify the level of performance degradation in the closed-loop control system in the presence of given perturbations. This *ad hoc* approach is not only time-consuming but also does not guarantee the system performance under untested perturbations. Alternatively, μ analysis provides a systematic approach to examine the frequency-domain performance robustness of perturbed systems.

The fundamental concept is to recast the robust performance problem into a robust stability problem [3], [6]. A fictitious block Δ_p is introduced into the uncertainty structure of the control system for robust performance evaluation where Δ_p specifies the desired relationship between exogenous disturbances and controlled plant variables. In this method, results from μ analysis can be used to determine the worst-case performance degradation associated with the specified perturbation. Subsequently, the μ synthesis technique can be used to construct a robust control law under the specified uncertainty and performance requirements.

In the μ synthesis problem, the performance requirements are specified by a weighting function $W_p(s)$. The zero fre-

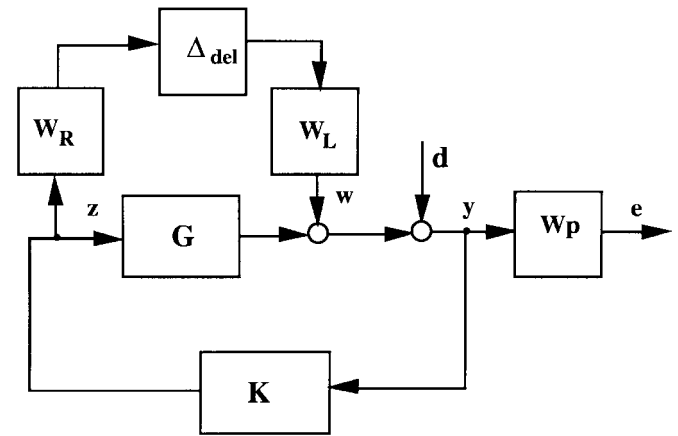


Fig. 3. Interconnection structure for robust feedback control analysis and synthesis.

quency response of $W_p(s)$ is set as follows:

$$(W_p(s=0))_{ij} = \frac{1}{\varepsilon_{ij}} \quad (10)$$

where ε_{ij} is the steady-state error in channel ij (i.e., from the j th input to the i th output). The interconnection structure of the synthesis problem in the robust performance setting is shown in Fig. 3. Most other time-domain performance cannot be directly specified in the frequency domain. Therefore, simulation experiments are needed for tuning the performance weighting matrices $W_p(s)$ in order to satisfy the time-domain performance requirements other than the steady-state error. The performance weighting matrix $W_p(s)$ and the associated structure Δ_p are specified as

$$W_p = \begin{bmatrix} \frac{0.7(s+1)}{s+0.1} & & & \\ & \frac{0.5(s+1)}{s+0.1} & & \\ & & \frac{0.5(s+1)}{s+0.1} & \\ & & & \frac{0.5(s+1)}{s+0.1} \end{bmatrix}$$

$$\Delta_p = \begin{bmatrix} \delta_{p11} & \delta_{p12} & \delta_{p13} & \delta_{p14} \\ \delta_{p21} & \delta_{p22} & \delta_{p23} & \delta_{p24} \\ \delta_{p31} & \delta_{p32} & \delta_{p33} & \delta_{p34} \\ \delta_{p41} & \delta_{p42} & \delta_{p43} & \delta_{p44} \end{bmatrix}. \quad (11)$$

The above specifications imply that the steady-state errors in each output channel are: electric power output (JGN) is $\sim 14\%$, throttle steam temperature (THS) is 20% , hot reheat steam temperature (THR) is 20% , and throttle steam pressure (PHS) is 20% , respectively. The full-block structure is specified for Δ_p to ensure that the steady-state errors of the regulated variables will satisfy the required level under perturbations in the reference input vector. For example, the steady-state error of the power output (JGN) due to perturbation in any one of the four control inputs is guaranteed not to exceed 14% of the difference in the respective power levels before and after the perturbation. That is, if the present load is 100% and the perturbation corresponds to a new load of 90% , then the steady state power after perturbation should be within $90 \pm 1.4\%$. The

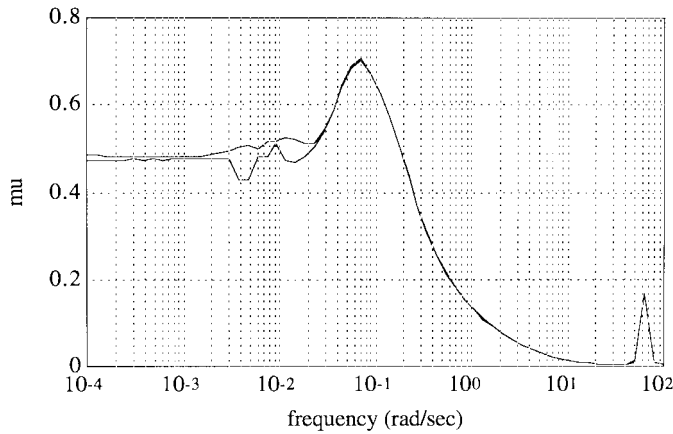


Fig. 4. The upper and lower bounds of μ for robust stability.

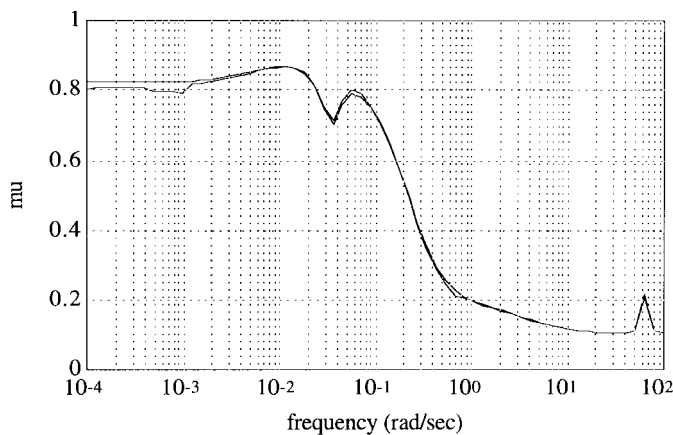


Fig. 5. The upper and lower bounds of μ for robust performance.

variations in valve dynamics represent the uncertainties due to neglected dynamics. Since the impact of errors in time constants die out as the system approaches the steady state, this uncertainty primarily affects the high-frequency components of the transient responses. On the other hand, a change in the turbine or pump efficiency influences the plant transients at all frequencies and has a strong bearing on the steady-state performance.

C. The FBC Law Based on the Linearized Plant Model

Since the physical process (i.e., the power plant) is operated in the continuous time, the measurements are sampled via A/D converters, and the discrete-time control signals are realized as continuous signals by using a zeroth-order hold via D/A converters. Such a system having both discrete and continuous signals is called a sampled-data system. Since the controller is designed and implemented in the discrete-time setting, this FBC synthesis problem belongs to the class of sampled-data systems. Consequently, the D-K iteration for μ -synthesis [6] is carried out by using the sampled-data H_∞ techniques based on the concept of lifting technique introduced by Bamieh and Pearson [1]. The FBC was synthesized for the sampling period of 0.1 s.

The computer software “MATLAB” and “ μ -Analysis and Synthesis Toolbox” were adopted to synthesize the feedback

controller. The resulting sampled data controller is of order 117 and satisfies the requirements of robust performance, after two D-K iterations. Figs. 4 and 5, respectively, show the μ -plots of robust stability and robust performance of the closed-loop control system in the frequency range of interest from 10^{-3} to 10^2 rad/s. The closed-loop performance plots are frequency weighted as described previously. Since robust performance implies that the system satisfies both stability and performance requirement in the presence of specified perturbations, as expected, the peak value of μ for robust stability is smaller than that for robust performance. In other words, in the event of increasing perturbations, the performance will degrade before the occurrence of instability. For robust stability, the peak value of μ in Fig. 4 is around 0.7, implying that the control system is guaranteed to be stable in the presence of uncertainties within approximately 140% of the specified bounds. Similarly, the largest value of μ in Fig. 5 is around 0.9, implying that the control system guaranteed to meet the performance requirements in the presence of uncertainties within approximately 110% of the specified bounds. That is, the closed-loop control system is guaranteed to remain stable and satisfy the performance requirements under the specified perturbations.

IV. RESULTS OF SIMULATION EXPERIMENTS

The FFC policy and the FBC law were combined to formulate the proposed integrated FF/FBC system. Under nominal conditions, i.e., no perturbation and uncertainties, the simulation results of the FF/FBC system for power decrease with no penalty on the variations of control inputs are shown in Figs. 6 and 7 for the transient responses of the plant output and input variables, respectively. Fig. 6 shows that, during the first 360 s for which the FFC was synthesized, there is no deviation between the actual trajectory and the optimal trajectory because no perturbation is injected into the nominal plant model. Therefore, during this period of 360 s, the FBC was inactive. However, after 360 s, the FFC inputs are held at the final values of the FFC sequence, which may not be identical to the steady-state control inputs corresponding to the terminal load. This is equivalent to injection of a disturbance at the instant of 360 s, and it is the responsibility of the FBC to maneuver and maintain the plant at the desired equilibrium point. The control system regulated deviations from the desired outputs and reached the steady state after ~ 15 minutes. The steady-state errors at outputs were observed to be: $\varepsilon_{\text{THS}} < 2^\circ\text{F}$ (1.1°C); $\varepsilon_{\text{THR}} < 3^\circ\text{F}$ (1.67°C); $\varepsilon_{\text{PHS}} < 6$ psi (0.0414 MPa); and $\varepsilon_{\text{JGN}} < 1$ MWe. Similar results for power ramp up are shown in Figs. 8 and 9.

A. The Control Systems Under Perturbations

In order to examine the performance of the control systems under perturbations, two types of parametric disturbances were injected. First, the time constant of each valve was made to be 1.5 times larger, that is, 50% error at each actuator dynamics. Physically, this means that the dynamics of the valve actuators are 50% slower than predicted by the model. Second, efficiency of the high-pressure turbines, intermedi-

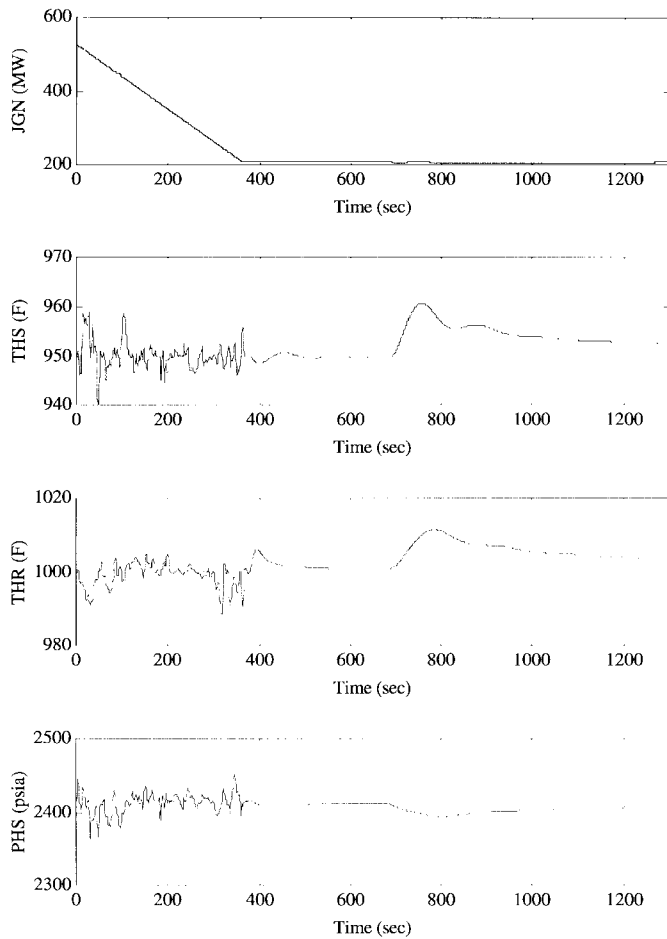


Fig. 6. Outputs of the FF/FBC system for power ramp down at 10%/min.

ate pressure turbines, and feedpumps were all reduced by 5%, that is, 5% modeling error, in these components. The variations in valve dynamics represent the uncertainties in modeling of the dynamic behavior. Since the impact of errors in time constants die out as the system approaches the steady state, this uncertainty primarily affects the high-frequency components of the transient responses. On the other hand, a change in the turbine or pump efficiency influences the plant transients at all frequencies and has a strong bearing on the steady-state performance. The simulation results of the FFC system alone (i.e., with no feedback action) under plant perturbations are shown in Fig. 10 in which solid lines represent the perturbed response and dotted lines represent the nominal FFC trajectories. The outputs are seen to deviate from the original respective optimized trajectories due to the injected perturbations. The variations in temperatures and pressure violate the specified constraints under the FFC alone. This implies that the throttle steam and hot reheat steam temperatures could not be maintained within the desired ranges without a robust feedback controller.

A major feature of the FF/FBC structure is that, in addition to the coarse control provided by FFC, FBC compensates for the deviations from the desired plant output trajectory by the fine-tuning control inputs. Perturbations identical to those injected into the FFC system were applied to the FF/FBC system to examine its robustness. Figs. 11 and 12,

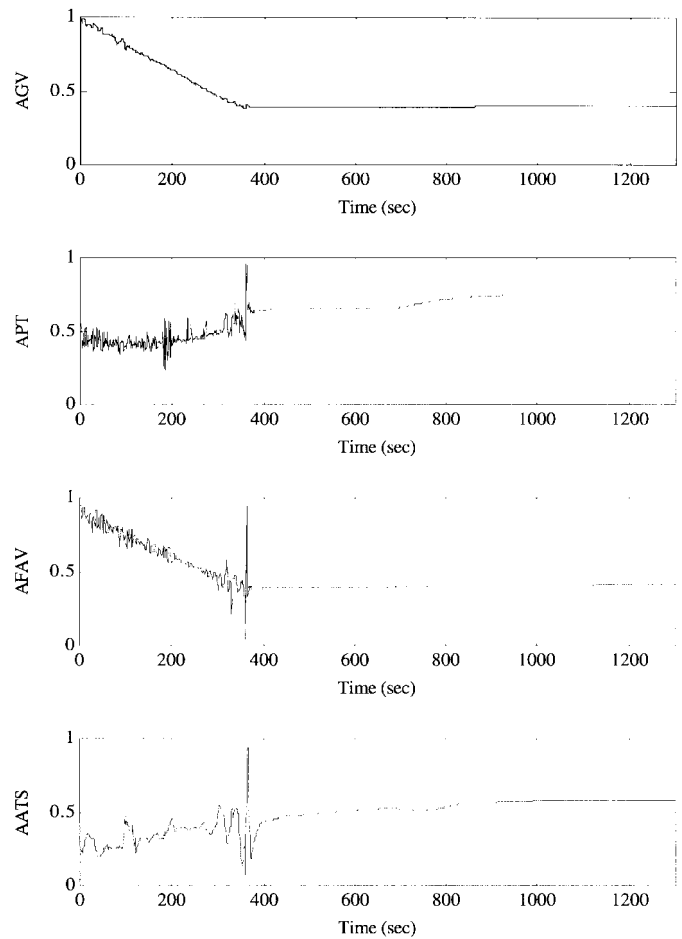


Fig. 7. Control inputs of the FF/FBC system for power ramp down at 10%/min.

respectively, show the output and input responses of the FF/FBC system for the first 360 s under these perturbations. Similar to Fig. 10, the perturbed responses and the nominal trajectories are represented by dotted lines and solid lines, respectively. It is seen in Fig. 12 that the control inputs were automatically adjusted by FBC to compensate for the deviations. As a result, in spite of the perturbations, the plant response closely followed the nominal optimized trajectory as seen in Fig. 11.

B. Implementation Issues of The Proposed FF/FBC System

To implement the proposed FF/FBC strategy on a plant, sets of FFC input and output sequences for different operating ranges should be precalculated and stored in the database of the control computer. The feedback control system alone can handle the load changes within a small operating range (e.g., 5% of full load). In that case, the FF/FBC system can be set up as a regulatory device under feedback control by setting the feedforward control input and output sequences, U^{ff} and Y^{ff} in Fig. 1, to respective fixed values as the reference signals. Therefore, only a finite number of FFC input and output sequences need to be stored in the database for different operating ranges; the desired operating range is not required to exactly conform to that for any one of the stored sequences.

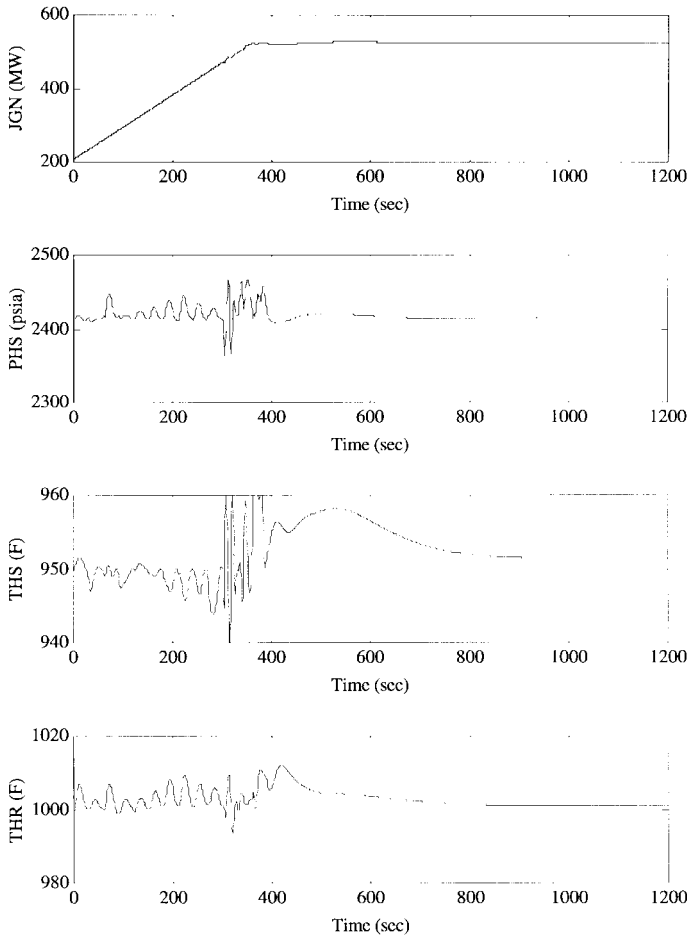


Fig. 8. Outputs of the FF/FBC system for power ramp up at 10%/min.

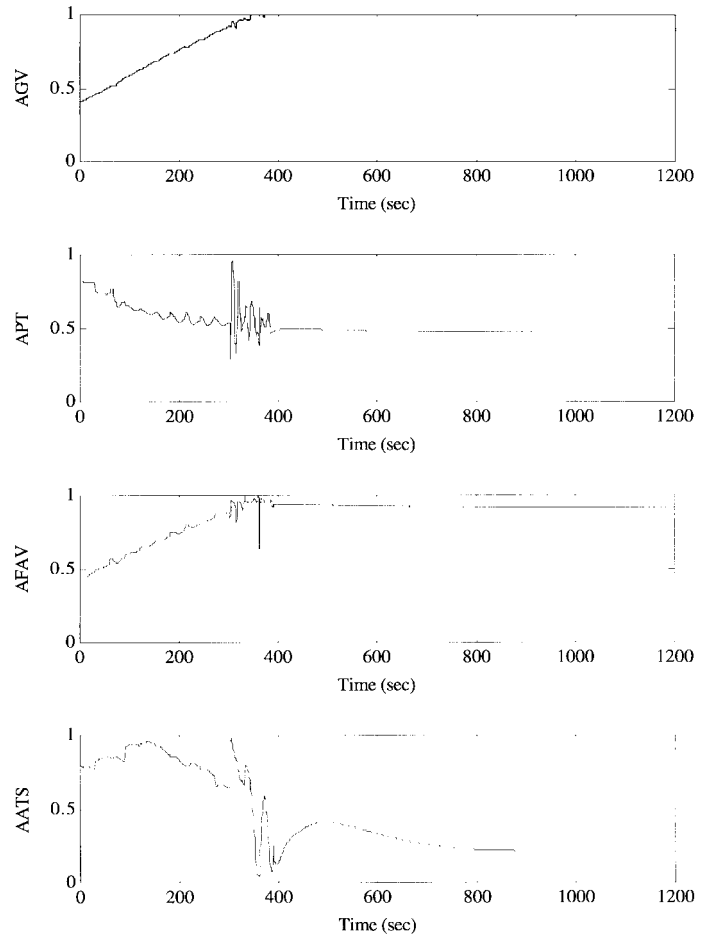


Fig. 9. Control inputs of the FF/FBC system for power ramp up at 10%/min.

The following three-step procedure, which can be executed on-line, is suggested as a general operation strategy.

- Step 1) Let the feedback controller maneuver the plant load to an operating condition which is close to the present operating point and correspond to the starting point of a stored set of sequences.
- Step 2) Let the FF/FBC maneuver the plant load close to the desired final state.
- Step 3) Let the FBC maintain the plant load at the desired steady-state point.

For example, let the current plant load be 87% of full power, and the load demand be required to be ramped down to 52%. Then, if a FFC policy starting from 85% is available in the database, the above procedure should be executed as follows:

Step 1: Apply the FBC alone to bring the plant load from 87% down to 85%.

Step 2: Apply the FF/FBC to ramp down the plant load from 85% to 52%.

Step 3: Apply the FBC alone to maintain the plant load at 52%.

V. SUMMARY AND CONCLUSIONS

This paper proposes a methodology for synthesizing an integrated FF/FBC strategy for robust wide-range control of

commercial-scale steam-electric power plants. In this methodology, the FFC policy is generated via nonlinear programming to provide optimized performance, and the FBC law is synthesized by the H_∞ -based structured singular value (μ) approach to achieve the desired stability and performance robustness.

Application of the proposed methodology is illustrated by synthesizing a control system for wide-range operations of a 525 MWe fossil-fueled electric power plant. For the purpose of control synthesis, the power plant is modeled in deterministic setting consisting of 27 state variables with four valve control commands selected as the plant inputs, namely, *fuel/air valve*, *feedpump speed control valve*, *turbine governor valve*, and *reheat spray attenuator valve*. The measured plant output variables are *electric power*, *main steam temperature*, *main steam pressure*, and *hot reheat steam temperature*. The synthesis of the FFC policy is identified as an optimal performance problem characterized by rapid maneuvering of electric power while maintaining the remaining three output variables as close as possible to their respective constant desired values. The FBC synthesis is posed as a multivariable control problem where the objective is to achieve robust stability and robust performance under specified performance criteria and uncertainty bounds, which represent errors due to linearization of the nonlinear plant model, unmodeled dynamics, and inaccuracy of the plant model parameters.

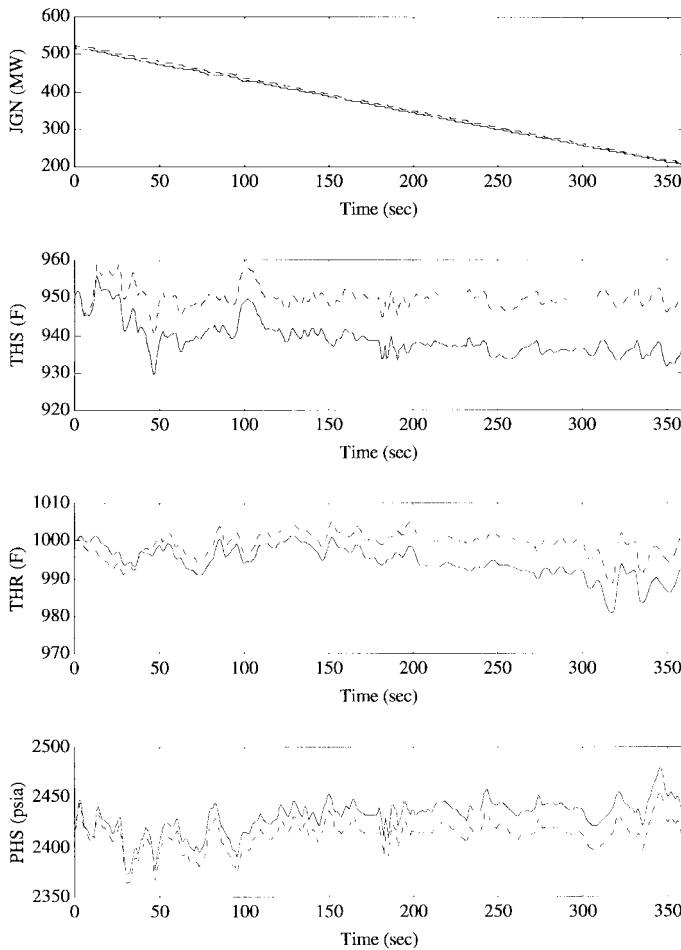


Fig. 10. Outputs of the FFC system under perturbations.

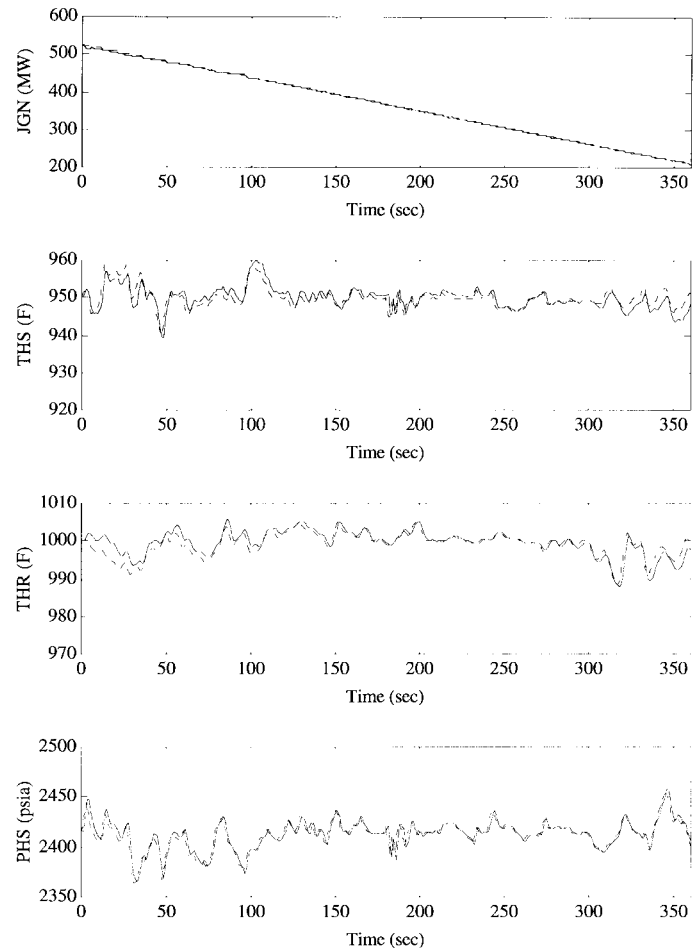


Fig. 11. Outputs of the FF/FBC system under perturbations.

The efficacy of this control synthesis methodology was investigated by simulation studies in which the synthesized FF/FBC law was applied to maneuver the nonlinear model of the power plant by ramping up and down the load in the range of 100% to 40% of the full power at the rate of 10% per minute. The results of simulation experiments showed that, under no plant modeling uncertainties, the FF/FBC system is able to satisfy the desired load maneuvering (i.e., 52.5 MWe/min up and down) while the main steam temperature, reheat steam temperature, and main steam pressure are maintained within $\pm 10^\circ\text{F}$ (5.56°C), $\pm 15^\circ\text{F}$ (8.33°C), and ± 45 psi (0.310 MPa), respectively. Simulated disturbances, representing plant modeling error and parametric uncertainties, were injected into the control system to investigate its robustness properties. Typically, these injected disturbances included parametric errors such as time constants of control valves and efficiency characteristics of the main steam turbines and the feedwater pump, which represent errors in the entire frequency range of the plant model. The simulation results suggest that the FBC is capable of rejecting the anticipated disturbances so that the plant could closely follow the optimal trajectory determined by the FFC policy.

In addition to these simulation studies, the proposed FF/FBC synthesis approach has been experimentally verified via on-

line operations on the TRIGA nuclear reactor at The Pennsylvania State University, University Park, PA [13]. The experimental results show that the FF/FBC controller is capable of maneuvering the reactor power as desired while the overshoot of the fuel temperature is suppressed to avoid any potential core damage.

Although this paper focuses on wide-range control and operation of fossil power plants, the FF/FBC strategy is also applicable to other complex processes such as planned shutdown of nuclear power plants, takeoff and landing of aircraft, and start-up and transient operations of rocket engines.

The major advantages of the proposed FF/FBC strategy, synthesized via the techniques of nonlinear programming and structured singular value, are delineated below:

- The methodology of FF/FBC synthesis is superior to the traditional approach of integrated control systems (ICS) synthesis in the sense that the optimal trajectory is known *a priori* by off-line nonlinear programming and that the robust feedback controller is only responsible for on-line compensation of small deviations from the desired trajectory.
- Nonlinear constraints in the time-domain setting can be conveniently specified in the nonlinear programming in the FFC synthesis, whereas the uncertainties that can be

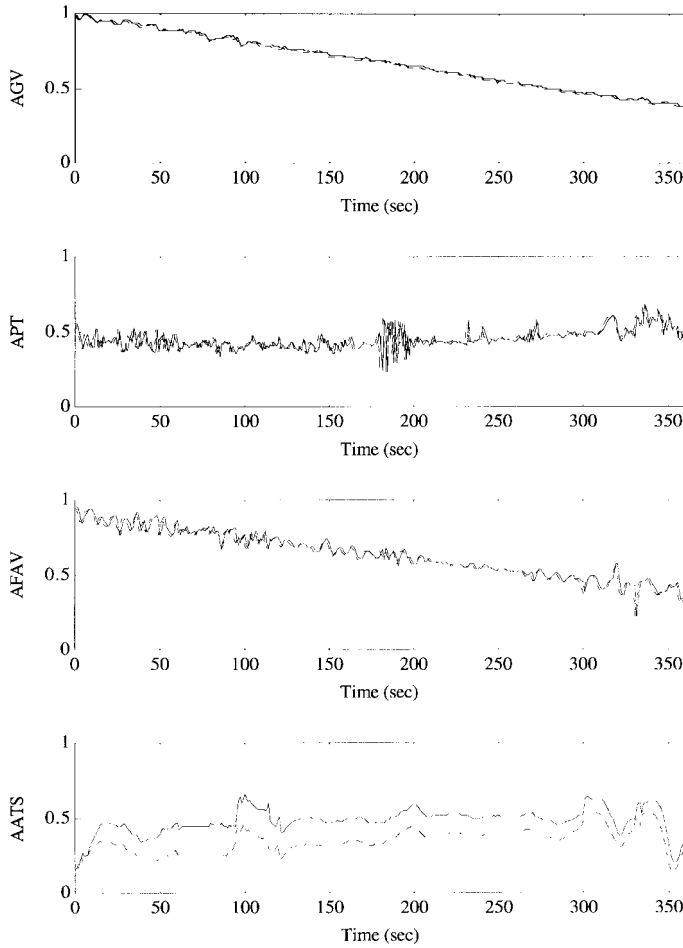


Fig. 12. Control inputs of the FF/FBC system under perturbations.

bounded in the frequency domain are dealt with in the FBC synthesis.

- The μ -synthesis guarantees robust stability and robust performance of the closed-loop control system under specified performance criteria and uncertainty bounds. No *ad hoc* testing of the closed-loop control system is necessary.

APPENDIX

THE STRUCTURED SINGULAR VALUE (μ)

The problem of robust control synthesis via μ is generally formulated in terms of the models of the nominal plant, the associated uncertainties in plant modeling, external disturbances, and the performance specifications [6]. Fig. 13 shows how the plant perturbations $\Delta(s)$ interact with the finite-dimensional linear time-invariant control system $M(s)$ which includes the plant $G(s)$ and the controller $K(s)$. The input w to the control system $M(s)$ consists of all exogenous signals, namely the reference command(s), disturbances and sensor noise; and the feedback control input. The output z of the control system consists of all plant variables needed for specifying the stability and performance criteria and the sensor data feeding the controller. In the definition of the structured singular value $\mu_{\Delta}(M(s_0))$ of the transfer matrix $M(s)$ at a

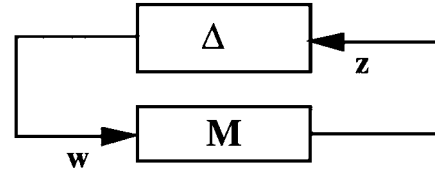


Fig. 13. The interconnection structure.

given s_0 , the underlying uncertainty $\Delta(s)$ belongs to a set of matrices $\underline{\Delta}(s)$ which is prescribed to have a block diagonal structure with the three characteristics: 1) type of each block; 2) total number of blocks; and 3) dimension of each block.

In general, there are two types of blocks: repeated scalar blocks and full blocks. Let two nonnegative integers, S and F , represent the number of repeated scalar blocks and the number of full blocks, respectively. Two sets of positive integers, r_1, r_2, \dots, r_S and m_1, m_2, \dots, m_F , are used to represent the dimensions of these blocks such that

- the i th repeated scalar block is $\delta_i I_{r_i}$ where I_{r_i} is the identity matrix and $\delta_i \in \mathcal{C}$
- the j th full block belongs to $\mathcal{C}^{m_j \times m_j}$.

The block diagonal structure $\underline{\Delta}(s)$ is defined as

$$\underline{\Delta}(s) = \{\text{diag}[\delta_1(s)I_{r_1}, \dots, \delta_S(s)I_{r_S}, \Delta_1(s), \dots, \Delta_F(s)]: \delta_i \in \mathcal{C}, \Delta_j \in \mathcal{C}^{m_j \times m_j}\} \quad (12)$$

where

$$\sum_{i=1}^S r_i + \sum_{j=1}^F m_j = n.$$

For any $M \in \mathcal{C}^{n \times n}$, its structured singular value $\mu_{\underline{\Delta}}(M)$ is defined as [3]

$$\mu_{\underline{\Delta}}(M) \equiv \left\{ \frac{1}{\inf\{\bar{\sigma}(\Delta): \Delta \in \underline{\Delta}, \det(I - M\Delta) = 0\}} \mid \forall \Delta \in \underline{\Delta}, \det(I - M\Delta) \neq 0 \right\} \quad (13)$$

REFERENCES

- [1] B. A. Bamieh and J. B. Pearson, "A general framework for linear periodic systems with applications H_{∞} to sampled-data control," *IEEE Trans. Automat. Contr.*, vol. 37, pp. 418–435, 1992.
- [2] E. J. Brailey, H. L. Miller, and C. G. Sterud, "Control valves limit turbine temperature swings," *Power Eng.*, vol. 95, no. 4, 1991.
- [3] J. C. Doyle, "Analysis of feedback systems with structured uncertainties," *IEE Proc.*, vol. 129, Part D, no. 6, 1982, pp. 242–250.
- [4] C. F. Gerald and P. O. Wheatley, *Applied Numerical Analysis*, 3rd ed. Reading, MA: Addison-Wesley, 1984.
- [5] P. E. Gill, W. Murray, M. A. Saunders, and M. H. Wright, *User's Guide for NPSOL (Version 4.0): A Fortran Package for Nonlinear Programming*, Stanford Univ., CA, 1986.
- [6] A. Packard and J. C. Doyle, "The complex structured singular value," *Automatica*, vol. 29, pp. 71–109, 1993.
- [7] A. Ray and D. A. Berkowitz, "Design of a practical controller for a commercial scale fossil power plant," *ASME J. Dynamic Syst., Measurement, Contr.*, Dec. 1979, pp. 284–289.
- [8] A. Ray and C.-K. Weng, "Robust wide-range control of steam-electric power plants," Electric Power Res. Inst., Palo Alto, CA, Rep. Contract EPRI RP 8030-5, Dec. 1994.
- [9] K. Schittkowski, "Software for mathematical programming," in *Computational Mathematical Programming*. New York: Springer-Verlag, 1985.

- [10] D. J. Smith, "Instrumentation and control systems are going state-of-the-art," *Power Eng.*, vol. 97, no. 11, 1993.
- [11] S. C. Stultz and J. B. Kitto, Eds., *Steam, Its Generation and Use*, 40th ed. Barberton, OH: Babcock and Wilcox, 1992.
- [12] E. Wasil, B. Golden, and L. Liu, "State-of-the-art in nonlinear optimization software for the microcomputer," *Computers Operations. Res.*, vol. 6, pp. 497-512, 1989.
- [13] C-K. Weng, "Robust wide-range control of electric power plants," Ph.D. dissertation, The Pennsylvania State Univ., University Park, PA, 1994.
- [14] C-K. Weng, M. Power, R. M. Edwards, and A. Ray, "Feedforward-feedback control by nonlinear programming and structured singular value approach," in *Proc. ANS Winter Mtg.*, Washington, D.C., Nov. 1994.

Chen-Kuo Weng received the M.S. and Ph.D. degrees in mechanical engineering from the Pennsylvania State University, University Park, PA, in 1993 and 1994, respectively.

His research experience and interests include robust control systems and optimization of continuously varying dynamic systems as applied to power plants.

Asok Ray (SM'83) received Master's degrees in electrical engineering, computer science, and mathematics, and the Ph.D. degree in mechanical engineering from Northeastern University, Boston, MA, in 1976.

He held research and academic positions at the Massachusetts Institute of Technology, Cambridge, and Carnegie-Mellon University, Pittsburgh, PA, as well as research and management positions at GTE Strategic Systems Division, Charles Stark Draper Laboratory, and MITRE Corporation. He joined the Pennsylvania State University, University Park, in July 1985, and is currently a Professor of Mechanical Engineering. His research experience and interests include modeling and analysis of thermo-mechanical fatigue and creep, intelligent instrumentation for real-time distributed processes, fault-accommodating and robust control systems, and control and optimization of continuously varying and discrete-event dynamic systems in both deterministic and stochastic settings, as applied to undersea autonomous vehicles, aircraft and spacecraft, and power plants. He has authored or coauthored more than 250 research publications including more than 100 scholarly articles in refereed journals, and also a research monograph, *An Integrated System for Intelligent Seam Tracking in Robotic Welding* (London: Springer-Verlag).

Dr. Ray is a Fellow of ASME and an Associate Fellow of AIAA. He was an Associate Editor of the *Journal of Dynamic Systems, Measurement, and Control* and *Transactions of the American Society of Mechanical Engineers*, and is an Associate Editor of *International Journal of Flexible Manufacturing Systems*. He is also a Registered Professional Electrical Engineer in the Commonwealth of Massachusetts.